VLBI Observations of GNSS Signals on the Baseline Hobart–Ceduna

First Results

Andreas Hellerschmied[1], Johannes Böhm[1], Younghee Kwak[1], Jamie McCallum[2], Lucia Plank[2]

Abstract Observing GNSS satellites with geodetic VLBI opens a variety of new possibilities, which include promising applications in the field of inter-technique frame ties. Considering GNSS satellites as co-location platforms in space, such observations provide possibilities to directly connect the dynamic GNSS and the kinematic VLBI reference frames, which may result in improved future ITRF realizations. In our research we are trying to apply observation strategies that are commonly used in geodetic VLBI, i.e., the main observables are group delays derived from direct observations of GNSS satellite signals. However, clear strategies for the data acquisition and the geodetic analysis are still missing. To pave the way towards an operational application we established a workflow to plan, correlate, observe, and analyze VLBI observations to GNSS satellites. Based on these processes we carried out several successful experiments on the Australian baseline Hobart–Ceduna in 2015 in which we observed GLONASS and GPS satellites in the L1 and L2 bands. For the first time a connected processing chain from scheduling, to correlation, to data analysis has been realized. In this contribution we introduce our workflow and present first results.

Keywords VLBI satellite observations, GNSS, VieVS

1. Technische Universität Wien, Austria
2. University of Tasmania, Australia

1 Introduction

The use of co-location platforms in space for the realization of frame ties between the key space-geodetic techniques, as a supplement to the earthbound localties, is a hot topic in the geodetic community. As dedicated satellite missions, such as the GRASP mission proposed in 2011 (Nerem & Draper, 2011), are rare and not suitable for extensive testing, VLBI observations to GNSS satellites provide a promising alternative to connect the dynamic GNSS and the kinematic VLBI reference frames. In a broader context, observations of GNSS satellites can also be considered as a preparation for observations to future dedicated co-location satellites, such as E-GRASP or E-GRIP (Männel *et al.*, 2016).

In our research we focus on direct observations of GNSS satellite signals with the geodetic VLBI system, trying to apply observation schemes which are commonly used in geodetic VLBI. Hence, our main observables are group delays derived from direct observation and subsequent correlation of GNSS satellite signals, which are treated in the geodetic analysis similarly to delays derived from standard observations of quasars.

Compared to previous experiments carried out within recent years (e.g., Tornatore *et al.*, 2014; Hellerschmied *et al.*, 2014) we also incorporated the correlation, fringe fitting, and analysis in one seamless processing chain. In this paper we first introduce the established workflow and then show initial results for actual GNSS observations on the baseline Hobart–Ceduna (Australia) carried out in 2015.

2 Observations

2.1 Scheduling

The starting point of each VLBI session is a precise observation schedule, defining which sources are observed by which antennas at a given time. The scheduling of satellite observations is a complex task, taking into account numerous observation restrictions caused by the observation geometry, satellite orbit characteristics (e.g., low orbit altitude restricts the common visibility from widely separated stations) and antenna capabilities (e.g., tracking features, slew rate limits, observable frequency range).

For the scheduling of the GNSS observations the VieVS satellite scheduling program (Hellerschmied *et al.*, 2015) was used, which is included as a module in the Vienna VLBI Software (VieVS; Böhm *et al.*, 2012). Basically, it is a convenient tool for the scheduling of real VLBI satellite observations and the creation of the required VEX-formatted schedule files. The orbit determination is based on Two-Line Element (TLE) data sets, which are widely available online. The program also allows generation of combined schedules with observations of satellites and natural sources within one session. The station-specific VEX files can then be used to control GNSS VLBI sessions in an automated manner.

This tool was used to schedule the experiments listed in Table 1 for the baseline Hobart–Ceduna (see Section 2.2) in 2015. During all sessions GLONASS and GPS satellites were observed in the L1 and L2 bands, along with some quasars for calibrations.

2.2 Observation Network

All discussed observations were carried out by the 26-m antenna at Hobart (Ho), Tasmania, and the 30-m antenna at Ceduna (Cd), South Australia, realizing a single baseline of ∼1,700 km length. Both antennas were equipped with linearly polarized (X and Y) L-band receivers with a nominal operating range from 1.35 to 1.65 GHz. Although the GNSS L2 signals (GPS: 1227.6 MHz; GLONASS: 1246.0 MHz) were out of the nominal receiver range and therefore attenuated, a signal reception was still possible due to the high power level of the observed signals.

Table 1 GNSS VLBI experiments on the baseline Ho–Cd in 2015.

Exp. name	Date	Dur.	Obs. GNSS	Sat. scans
g179a	2015-06-28	2h	GPS, GLONASS	13@5min
g236a	2015-08-24	4h	GPS	23@5min
g238a	2015-08-26	4h	GPS, GLONASS	23@5min

To keep track of the moving satellites during data acquisition, a so-called stepwise satellite tracking approach (described in detail by e.g. Hellerschmied *et al.*, 2015) was implemented in the observation schedules. Basically, satellite orbits are converted to sequences of discrete positions defined by topocentric right ascension and declination. These station dependent tracking points are then used to track the satellites by repositioning the antennas—virtually stepwise—in a time interval of 10 seconds. The recording of data is practically continuous.

2.3 The 'g236a' Experiment

As a representative example we describe one of the sessions observed in 2015, the 'g236a' session, in detail. First results are presented in the following sections. The g236a experiment was carried out on August 24 from 12:00 to 16:00 UTC. Four GPS satellites (PRN: 02, 12, 24, 24) were observed along with two natural sources (1921–293 and 0208–512). Data was recorded in four 16-MHz channels, centered at the L1 and L2 GPS carrier frequencies, respectively, X- and Y-polarized in each case ($L1_x$, $L1_y$, $L2_x$, $L2_y$).

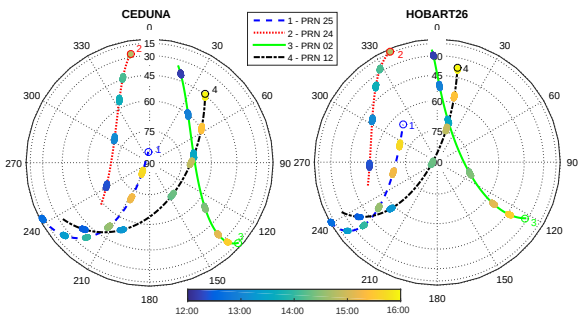

Fig. 1 Skyplots for the participating stations of the 'g236a' experiment (August 24, 2015; 12:00–16:00 UTC).

The scan sequence is illustrated in the skyplots for Ho and Cd in Figure 1. Satellites were observed in scans of five minute duration each, switching the observation target after each scan. With this configuration each satellite was observed in several scans well-distributed over the visible arcs. In Figure 1 the observation time is color-coded. Single quasar scans were scheduled roughly every hour between the satellite scans and at the start and end of the session.

3 Correlation and Fringe Fitting

For the correlation (input model) and the data analysis we needed the ability to calculate near field a priori delays for the VLBI observations of GNSS satellites. Therefore, VieVS was upgraded with a near field delay model (Plank *et al.*, 2014), which implements an iterative solution of the light time equation applying relativistic corrections according to Klioner (1991). Satellite positions used for the delay modeling were interpolated from IGS final orbits[1].

The data was correlated with the DiFX software (Deller *et al.*, 2007). As the standard correlator input model generated by the supplied Calc-Server was designed for sources at a virtually infinite distance (e.g., quasars), we calculated dedicated near field delay models for the observed satellites in VieVS and entered them into the control files.

For fringe fitting the FRING task in AIPS and also Fourfit, which is the standard tool in geodesy, were applied successfully. The drawback of using FRING in AIPS for geodetic purposes is that the delay epochs are referred to the geocenter, rather than the signal reception at the first network station, which is the common practice in geodesy. On the other hand, AIPS provides more possibilities for manipulating and investigating the data than Fourfit.

The 'g236a' data presented in this paper was correlated with a 10 second integration time in DiFX. Therefore we derived one delay solution every 10 seconds within each satellite scan of five minute duration in total. The SNR values after fringe fitting in Fourfit were very high, with values larger than 7000 for the L1 data and between 500 and 700 for the L2 data. The SNR for the L2 data is lower, because these signals were out of the receiver range and therefore attenuated.

Figure 2 depicts fringe delays of the 'g236a' experiment calculated in AIPS. Fringe delays basically represent the deviation between actual observations and the a priori delays derived from the correlator input model. We calculated single band delays of the in-phase correlation products (XX and YY) of the recorded L1 and L2 channels. This results in four delay solutions ($L1_{XX}$, $L1_{YY}$, $L2_{XX}$, $L2_{YY}$) per solution epoch (10 second interval)—one per recorded channel (color-coded in Figure 2). As the delays are plotted versus observation time individual five minute scans can clearly be discerned. The RMS scatter within these five minute scans is in the range of several tens of ps. We find large systematic offsets between the recorded channels with up to 40 ns (e.g., in scan 20). Due to this issue a combination of the two recorded orthogonal polarizations (X, Y) was not successful so far. Hence, we only use the $L1_{XX}$ delays for our further discussions.

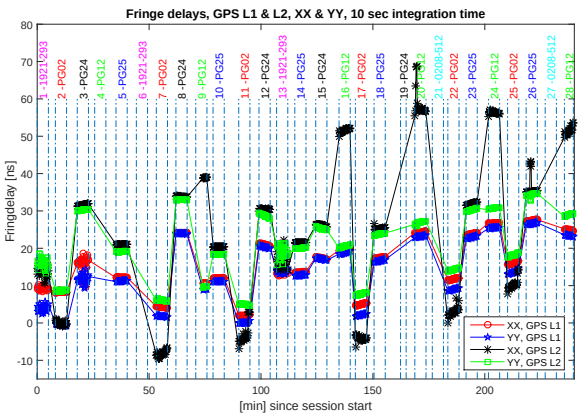

Fig. 2 Fringe delays of experiment 'g236a' calculated in AIPS. The names of the observed sources are shown in the top line. Delays for the natural sources (1921–293, 0208–512) are missing or noisy, because the applied 10 second integration time was too short for good results from these comparably weak sources.

4 Data Analysis

A preliminary data analysis was carried out in VieVS, based on single band group delays of the observed GNSS satellites calculated in Fourfit.

[1] https://igscb.jpl.nasa.gov/components/prods.html

Due to the systematic channel offsets ionospheric delay corrections could not be determined directly from the satellite observations in two bands (L1+L2) so far. Alternatively, ionospheric corrections for all observations were calculated from Global Ionospheric Maps (GIM, e.g., IGS TEC maps[2]) using dedicated functions in VieVS (Tierno Ros *et al.*, 2011). For the 'g236a' experiment these corrections were in a range between 1 and 5 ns.

Figure 3 depicts observed minus computed (O–C) values calculated for satellite observations in the 'g236a' experiment. O–C values are used as input for a subsequent least-squares adjustment. The observed values (O) are calculated as fringe delays from the $L1_{XX}$ correlation products plus a priori delays from the correlator input model (= total delays). Computed values (C) were calculated with near field delay modeling in VieVS (see Section 3). All O–C values range from -1 to $+4$ ns. In the O–C plot the tracks of the four observed satellites show characteristic signatures with variations between 1 and 4 ns per track. Underlying reasons for these satellite track signals and the O–C offsets in general (e.g., model inaccuracies, clocks, troposphere) are still the subject of investigations. Within individual five minute scans the accuracy is quite good at this point with an RMS scatter between $\sim$10 and 100 ps. Figure 4 depicts two scans (8 and 23) in detail.

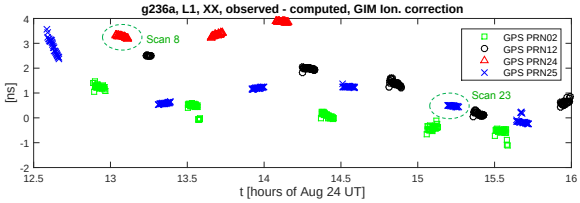

Fig. 3 Observed-minus-computed values for satellite observations of the 'g236a' experiment. Scans 8 and 23 are shown in detail in Figure 4.

Based on the O–C values described above we estimated clock parameters for Ho using least-squares adjustment in VieVS. Estimated parameters were hourly piece-wise linear offsets, one rate, and one quadratic term. The resulting post-fit residuals are shown in Figure 5. They are in a range of $\pm$50 cm, and the post-fit weighted RMS is 29.6 cm. In principle VieVS is able to estimate further geodetic parameters based on VLBI satellite observations analogous to the analysis of standard geodetic VLBI sessions with observations of natural sources. However, at this point the residuals between observations and theoretical delays are still quite large as shown above. Therefore, our preliminary conclusion is that observations and models have to be improved to be able to estimate further parameters (e.g., tropospheric zenith wet delays) meaningfully.

[2] https://igscb.jpl.nasa.gov/components/prods.html

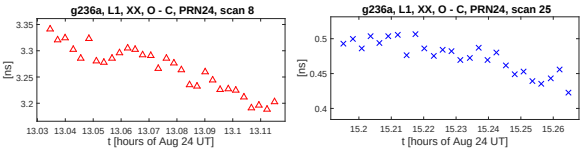

Fig. 4 Observed-minus-computed values of scans 8 and 23 of the 'g236a' experiment.

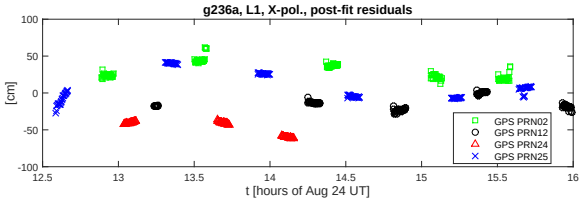

Fig. 5 Post-fit residuals of satellite observations during the 'g236a' experiment (WRMS = 29.6 cm).

5 Summary and Outlook

We established a processing chain to plan, observe, correlate, and analyze VLBI near field observations to (GNSS) satellites. For the scheduling the VieVS satellite scheduling module was used, providing convenient features for creating VEX files for satellite observations. Furthermore, VieVS was upgraded with a near field delay model to calculate a priori delays for GNSS satellite observations. Additional modifications allow VieVS to input delay observables from satellite observations and to use them as the basis for geodetic analysis and parameter estimation. DiFX was used for correlations, applying dedicated correlator input models for near field observations calculated directly in VieVS. For the fringe fitting we successfully applied both AIPS and Fourfit, the latter being the standard tool in geodesy.

The VLBI antennas at Ceduna and Hobart, which are directly operated by the University of Tasmania (UTAS), are a great test bed for VLBI satellite observations, because they are equipped with L-band receivers, capable of recording GNSS L1 and L2 signals.

Based on the introduced workflow we carried out several successful GNSS VLBI experiments in June and August 2015 on the baseline Ho–Cd. For the 'g236a' experiment, which was discussed as a representative example, the resulting post-fit WRMS was 29.6 cm after estimating clock parameters in VieVS. Although the residuals are still quite large, it shows that our observation and analysis schemes in principle work. Currently, the main issues are the elimination of systematic offsets between the recorded channels and the rigorous combination of the recorded X- and Y-polarized signals to get one single and unambiguous delay for the L1 and L2 band per solution epoch.

Nevertheless, these observations for the first time combined all steps in a connected processing chain: scheduling (including the provision of VEX files for the observation and correlation), the creation of correlator input models, the derivation of total delays, and finally the actual data analysis. This workflow tremendously eases the implementation of such VLBI observations of GNSS satellites, opening up the field for further investigations and improvements.

Acknowledgements

This work was supported by the Austrian Science Fund (FWF, projects I2204 and J3699-N29).

References

BÖHM, J., BÖHM, S., NILSSON, T., PANY, A., PLANK, L., SPICAKOVA, H., TEKE, K., AND SCHUH, H. (2012). The New Vienna VLBI Software VieVS. In S. Kenyon, M. C. Pacino, and U. Marti, eds., *Geodesy for Planet Earth*, Vol. 136 of *International Association of Geodesy Symposia*, 1007–1011, Springer Berlin Heidelberg.

DELLER, A., TINGAY, S., BAILES, M., AND WEST, C. (2007). DiFX: A Software Correlator for Very Long Baseline Interferometry Using Multiprocessor Computing Environments. *The Publications of the Astronomical Society of the Pacific*, 119, 318–336.

HELLERSCHMIED, A., PLANK, L., NEIDHARDT, A., HAAS, R., BÖHM, J., PLÖTZ, C., AND KODET, J. (2014). Observing satellites with VLBI radio telescopes - practical realization at Wettzell. In D. Behrend, K. Baver and K. Armstrong, eds., *IVS 2014 General Meeting Proceedings*, 441–445, Science Press (Beijing). ISBN 978-7-03-042974-2.

HELLERSCHMIED, A., BÖHM, J., NEIDHARDT, A., KODET, J., HAAS, R., AND PLANK, L. (2015). Scheduling VLBI Observations to Satellites with VieVS. In C. Rizos and P. Willis, eds., *Proc. IAG Commission 1 Symposium 2014: Reference Frames for Applications in Geosciences (REFAG2014)*, International Association of Geodesy Symposia, Springer Berlin Heidelberg, available online.

KLIONER, S. (1991). General Relativistic Model of VLBI Observables. In W. Carter, ed., *Proc. of AGU Chapman Conference on Geodetic VLBI: Monitoring Global Change, NOAA Technical Report NOS 137 NGS 49*, 188–202, American Geophysical Union, Washington D.C.

MÄNNEL, B., ROTHACHER, M., JETZER, P., LECOMTE, S., AND ROCHAT, P. (2016). E-GRIP: A Highly Elliptical Orbit Satellite Mission for Co-location in Space. In *Proceedings of the 9th IVS General Meeting, Johannesburg*, this volume.

NEREM, R.S. AND DRAPER, R.W. (2011). Geodetic Reference Antenna in Space. *GRASP proposal submitted in response to NNH11ZDA0120*, prepared for National Aeronautics and Space Administration Science Mission Directorate September 29, 2011.

PLANK, L., BÖHM, J., AND SCHUH, H. (2014). Precise station positions from VLBI observations to satellites: a simulation study. *J Geod*, 88, 659–673.

TIERNO ROS, C., BÖHM, J., AND SCHUH, H. (2011). Use of gnss-derived tec maps for vlbi observations. In *Proceedings of the 20th Meeting of the European VLBI Group for Geodesy and Astrometry, Bonn*, 114–117.

TORNATORE, V., HAAS, R., CASEY, S., POGREBENKO, S., AND MOLERA CALVÉS, G. (2014). Direct VLBI Observations of Global Navigation Satellite System Signals. In C. Rizos and P. Willis, eds., *Earth on the Edge: Science for a Sustainable Planet, Proc. IAG General Assembly, 2011*, Vol. 6 of *International Association of Geodesy Symposia*, 247–252, Springer Berlin Heidelberg.